2024 IEEE International Conference on Robotics and Automation (ICRA 2024)
May 13-17, 2024. Yokohama, Japan

A Dragonfly-inspired Flapping Wing Robot Mimicking Force Vector Control Approach

Fangyuan Liu[1], Song Li[1,2], Jinwu Xiang[1], Daochun Li[1], and Zhan Tu[1,3,*]

***Abstract*— Dragonflies show impressive flying skills by achieving both high efficiency and agility. They can perform distinctive flight maneuvers, such as flying backwards, which has proven to be achieved through "force vectoring" mechanism recently. In this paper, to explore the agile flight ability of dragonflies on man-made flapping wing systems, we designed, optimized and fabricated a dragonfly-inspired flapping wing robot (DFWR) with inclinable stroke plane control degrees. The proposed platform employs a four-wing configuration, each of which integrates an extra servo motor to enable the rotation of the flapping plane and imitate the "force vectoring" mechanism. Besides, referring to the flapping kinematics of dragonflies, the installation angle and wing pitch angle of the proposed DFWR are optimized considering the total lift and energy consumption through multiobjective optimization based on NSGA-II method. The "force vector" produced by the proposed platform has been illustrated through both theoretical method and experimental method. Moreover, the feasibility of the design is further verified through a series of operation validation experiments. Such a robot has the potential to provide a highly biomimetic platform to validate the flight mechanism studying of Odonata as well as the relative on-board applications such as bio-inspired vision.**

I. Introduction

Flapping wing micro aerial vehicles (FWMAV) have shown advantages in conquering challenges for small-scale propulsion of MAVs [1], and they have the potential to conduct environmental exploration and search and rescue missions, which are highly involved with the size or concealment of the aerial drones [2]–[5]. FWMAVs take inspiration from natural flying creatures, leveraging the unsteady aerodynamics, high lift, and high efficiency of flapping wing configuration at low Reynolds numbers [6], [7], effectively promising the propulsion efficiency of drones at miniature scales. Previous research has achieved many successful examples of transferring flying organism characteristics to robotic systems, dominated by mimicking the flapping flight of hummingbirds [5], [8], [9], beetles [10], flies [11], and birds [12]. However, state-of-the-art FWMAVs reported in the literature have not taken much inspiration from dragonflies, who have shown great flight ability in the nature due to their unique tandem flapping wing configuration [13].

There have been a few related works including BionicOpter invented by Festo Company which gave each wing multi degrees of freedom (DOFs) in flapping frequency, flapping amplitude, and wing stroke plane rotation [14], QV designed by the Georgia Institute of Technology which utilized flapping frequency modulate method among four wings to achieve flight control like a quadcopter craft [15], and Dielectric Elastomer Actuators (DEA) powered robotic dragonfly proposed by MIT research group [16]. Among current dragonfly-inspired robots, the research mostly focused on actuation mechanism design in tandemly arranged four-wing configurations, rather than further exploring or verifying the mechanisms of high maneuverability flight of dragonflies such as their reverse flight principles. As one most typical flight aerobatics of dragonflies, backward flight may offer important clues to the study of flight control strategies of both biological organisms and bio-inspired robotic platforms [17], [18]. Recent studies on the observation and the aerodynamics of dragonflies' backward flight have further uncovered the mechanism of this kind of maneuver [17], [19]–[21], based on which, "force vectoring" has been proven to be the main mechanism behind such a maneuver.

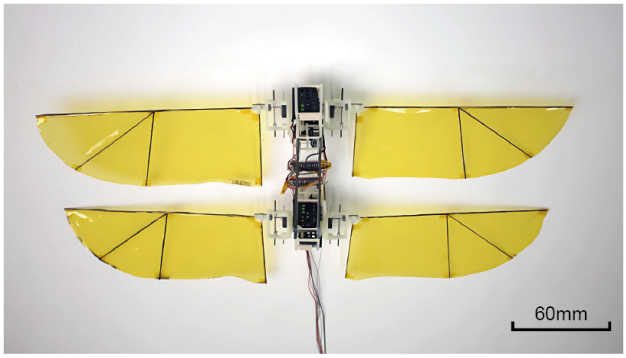

Fig. 1. Illustration of the proposed dragonfly-inspired flapping wing robot (DFWR) with "force vectoring" control mechanism.

Moreover, apart from replicating the propulsion mechanism of flyable creatures with miniature actuation systems for flapping wing motion [22], recent studies on FWMAVs have paid more and more attention to exploring some new control approaches to achieve high agile flight performance of robots [23]. Modulating flapping amplitude is one common way to adjust the control force and torque in robotic flapping wing platforms [3], [24], [25]. For traditional mechanically driven flapping robots, an effective control approach is to adjust the wing twist angle, by which means the local attack angle of wings can be modulated [5], [10]. Besides, the flapping frequency. Nowadays, more new and effective control approaches have been uncovered [26], [27], taking inspiration from the nature.

In this paper, in order to verify and mimic the "force vectoring" control approach of dragonflies, we design and

[1]These authors are with School of Aeronautic Science and Engineering, Beihang University, Beijing, China. [2] The author is also with Department of Biomedical Engineering, City University of Hong Kong, Hong Kong. [3] The author is also with Institute of Unmanned System, Beihang University, Beijing, China. * Email: zhantu@buaa.edu.cn.

fabricate a dragonfly-inspired flapping wing robot (DFWR), with the stroke plane inclination control degree. For the purpose of exploring the control effect of such a mechanism on DFWR, we derive theoretical expressions and conduct experiments on the control torque of our proposed DFWR. And finally, operation tests including a "force vectoring" mechanism validation test and a guided flight test are conducted to further verify the feasibility and application potential of the proposed design. The main contribution of this research lies in the verification of the bio-inspired "force vectoring" control mechanism on an artificial robotic platform, providing not only a new control approach but a relevant design for the current flapping wing robotics study.

The rest of the article is organized as follows. Section II introduces the design, and fabrication procedure of the proposed DFWR prototype. Section III shows the optimization of the flapping wing design based on NSGA-II method. Section IV presents the theoretical analysis and experiments of the bio-inspired "force vector" control mechanism. Section V demonstrates the operation of the "force vectoring" mechanism and guided flight validation of the proposed robotic dragonfly. Section VI summarizes this work.

II. Design and Fabrication of the Robotic Platform

A. Design of the dragonfly-inspired robot

The robotic platform has a dragonfly-inspired four-wing layout, as shown in Fig. 2A. The whole robot was mainly divided into two modules: a forewing module and a hindwing module, which were cross-connected through carbon fiber beams. Each module contains one actuation system, two tiltable flapping wing mechanisms, as well as 3D-printed supporting frames.

For actuation system, the flapping motion of the two wings are driven by a Brushless DC motor (AP03 7000KV) via a two-stage gearbox. As shown in Fig.2C, the output of the actuation shaft is transmitted to the left and right flapping mechanisms through two cranks respectively. The gearbox has a reduction ratio of 18:1, which includes a 9T gear on the motor, 54T gear on the output shaft, and a double layer gear (12T/36T) in the middle stage.

The tiltable flapping mechanism has an adjustable stroke plane during the flapping motion, which is to mimic the "force vector" principle in dragonfly flight maneuvers. As shown in Fig.2B, this flapping mechanism consists of a crank, a slider, a wing base, and the tiltable base. When the crank was driven by the actuation shaft, its end slides in the slide slot, thus driving the wing base for reciprocating motion. The tiltable base is connected to the actuation shaft through bearings, which reserves a rotation degree of freedom for tilting. The stroke plane of the flapping wing is determined by the tilting angle δ of the tiltable base, which is controlled by a servo motor with a one-stage gear (reduction ratio of 1:2).

In order to generate efficient lift force, a passive pitching motion mechanism was adopted at wing root. Fig. 2B illustrates this structure design. The leading edge of the wing was connected to the wing base by a sleeve bearing, which allowed

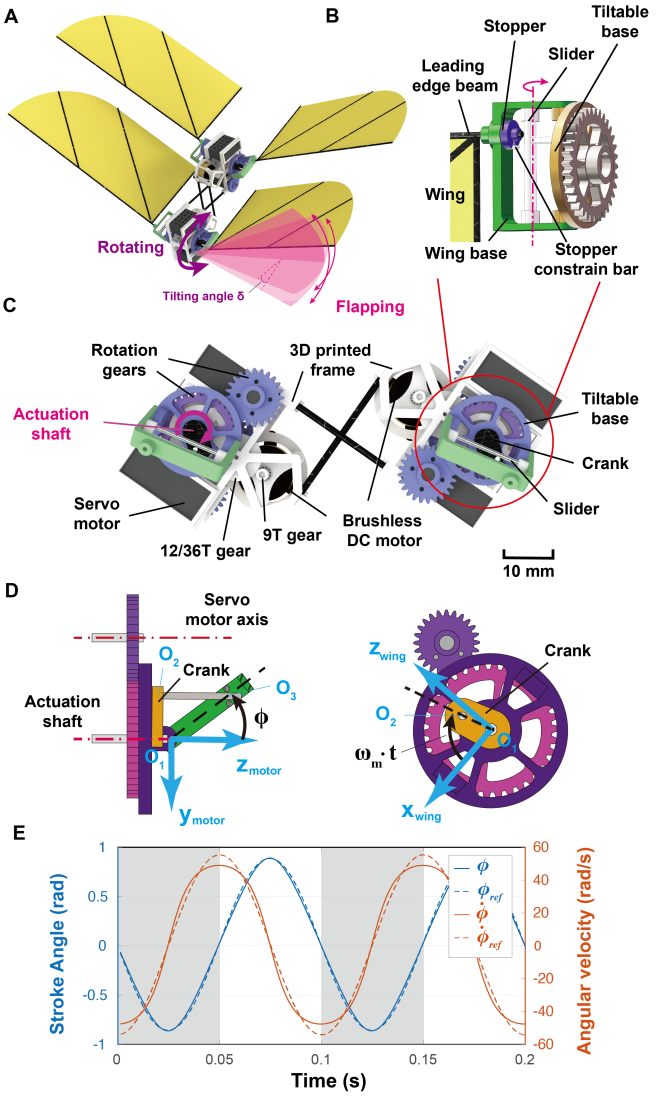

Fig. 2. Illustration of the design and kinematics of DFWR. (A) A prototype robot showing degrees of freedom of each flapping wing. Flapping wing structure design (B) and actuation components (C) ensuring the realization of "force vectoring" mechanism. (D) Parameters definition of the flapping wing kinematics model. (E) Comparison between the achieved Kinematics of flapping motion and standard sinusoidal curve.

the wing to rotate freely around its leading edge. Hence, the range of pitching angle was restricted by a stopper and a constrain bar, which are fixed on the wing and wing base respectively. The wings are fabricated by carbon fiber rods (diameter 0.9mm) and carbon fiber sheets (thickness 0.15mm). A 12um Polyimide (PI) film was cut as the wing membrane.

The total weight of the proposed DFWR is 36.10 grams. The mass distribution of each component is listed in table I.

B. Wing Kinematics

According to the flapping mechanism design, the kinetics of the flapping wing could be theoretically estimated. As shown in Fig. 2D, the rotation center of the crank is point O_1, the point the crank contacted with the slider is O_3. In $X_{wing}Z_{wing}$ plane, the crank continuously rotates around O_1 in one direction. Assuming the angular velocity is ω_m, the flapping angle ϕ can

TABLE I

MAIN COMPONENTS AND MASS DISTRIBUTION

Components	Quantity	Mass(g)
3D-printed supporting frame	2	3.78
Carbon fiber beams	4	2.14
Brushless DC motor	2	6.14
Gearbox for actuating	2	1.06
Actuation shaft	2	0.84
Bearings	8	0.64
Servo motor	4	11.44
Tiltable platform	4	2.76
Crank	4	0.68
Slider	4	0.70
Wing base	4	1.16
Wing with stopper	4	1.90
ESC and wires	2	2.86
Total mass		36.10

TABLE II

WING PARAMETER

Parameter	Symbol	Value	Unit
Non-dimensional radius	$\hat{r}_1^1$	0.4561	
Non-dimensional radius	$\hat{r}_2^2$	0.2805	
Non-dimensional radius	$\hat{r}_3^3$	0.1958	
Wing Span	R	140	mm
Short axis of the ellipse	a_2	65	mm
Maximum chord length	b	65	mm
Wing area	S	8.2×10^3	mm^2

be determined by

$$\phi = \arccos \frac{O_1O_2 \sin \omega_m t}{O_1O_3} \tag{1}$$

where O_1O_2 is the radius of the crank, O_1O_3 is also a predetermined constant of the wing base. In this way, the amplitude of the flapping motion can be turned by changing the value of O_1O_2 and O_1O_3.

The flapping angular velocity can be derived as

$$\dot{\phi} = -\frac{O_1O_2/O_1O_3\omega_m \cos(\omega_m t)}{\sin \phi} \tag{2}$$

Assuming that the motor speed ω_m is constant, the variation of flapping angle and its angular velocity within one period can be obtained through equation (1) and (2), as shown in figure 2E. At the same time, the standard sine function with the same flapping amplitude and frequency was also plotted as a reference value $\phi_{ref}, \dot{\phi}_{ref}$.

As shown in Fig. 2E, the flapping angle and its angular velocity are similar to standard sine curves (dashed lines). Although the maximum angular velocity is smaller than the reference value, it is worth noting that the changing trend of flapping angular velocity is relatively smooth near the peak value.

III. DESIGN OPTIMIZATION

In this section, the installation angle and wing pitch angle (reverse angle) of the proposed dragonfly-inspired flapping wing vehicle are optimized, aiming at a bigger lift force as well as a lower energy consumption during hovering flight respectively. To solve this multi-objective optimization problem, NSGA-II method is implemented based on a quasi-steady aerodynamic model of dragonfly-inspired wings.

A. Design Parameters

The flapping kinematics of dragonflies has been widely observed in earlier research, in which the pitch angle of wings and its changing patterns during a flapping stroke are regarded as vital parameters influencing the flight performance of free-flight dragonflies [28]–[30]. Specifically, the pitch angle pattern of our dragonfly-inspired robots can be adjusted by the installation angle and reverse angle (as shown in Fig.3(A)).

In order to establish the theoretical model for optimization, the detailed definition of these design parameters and the wing morphology are illustrated as follows.

*1) **Installation Angle**:* The installation angle refers to the angle between the wing base plane and the middle position of wing plane while flapping (wing mid-plane)(Fig.3(A))).

*2) **Reverse Angle**:* The reverse angle refers to the angle between the wing plane at the top position of a flapping stroke and the bottom position of a flapping stroke(Fig.3(A)).

*3) **Wing morphology**:* To enhance the time and resource efficiency of the optimization process, the wing is assumed to be a two-dimensional rigid thin plate [31], [32], and the wing morphology of the proposed dragonfly-inspired robot is shown at the bottom of Fig.3(A). Each wing is composed of a rectangular and 1/4 ellipse. The origin of the wing coordinate $O_wR_wC_w$ is located at the wing root, and O_wR_w axis and O_wC_w axis are along the leading edge and wing chord respectively. Hence, the length of wing chord at the location r can be expressed as:

$$c(r) = \begin{cases} b, & 0 \le r \le a_1 \\ \sqrt{b^2 - \frac{b^2}{a_2^2}(r-a_1)^2}, & a_1 < r \le R \end{cases} \tag{3}$$

in which a_1, b denote the length and width of the rectangular geometry; a_2 is the short axis of the ellipse; the half wingspan of the dragonfly-inspired wing is $R = a_1 + a_2$.

B. Objective Function

The goal of this design optimization process is to navigate the most proper design parameters including the installation angle and reverse angle of the wings, and to uncover the best flight performance of the proposed dragonfly-inspired robot in terms of both lift production and energy consumption.

To establish a theoretical model reflecting the lift production and energy consumption during the dragonfly-like flapping motion, the blade-element method is used in our work, in which the aerodynamic force acting on the wing plane is assumed as the summation of force acting on each span-wise strip at the location $R_w = r$ as shown in Fig.3(A). Thus, the total lift can be expressed as the integration of aerodynamic forces on each strip from the wing root to the wing tip:

$$F_{aero} = \int_0^R \frac{1}{2}\rho v_{local}^2 C_F(\alpha_{local}) C(r) \mathrm{d}r \tag{4}$$

where v_{local} and α_{local} respectively denote the local velocity and attack angle at the strip $R_w = r$. The local velocity v_{local} is composed of the flapping velocity v_f and air velocity v_{in} (the v_{in} equals to 0 in hovering situation in this work), the

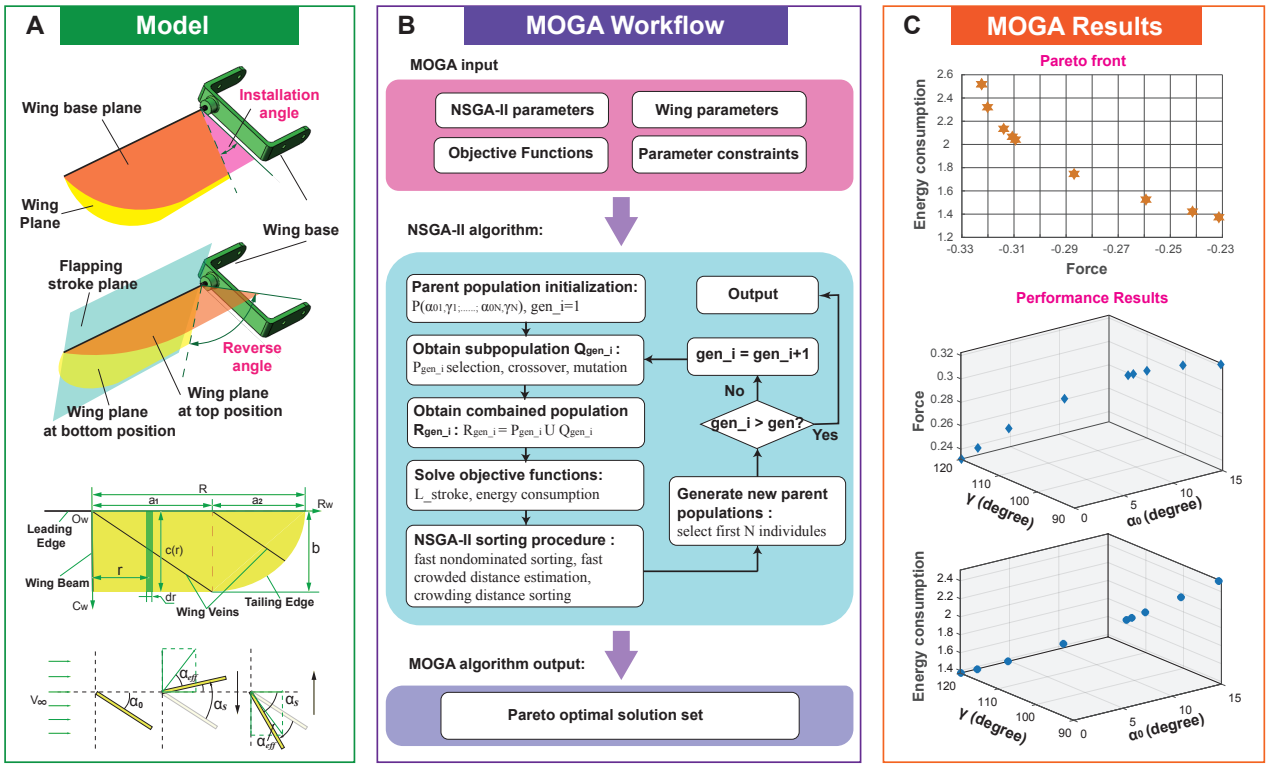

Fig. 3. Illustration of the optimization procedure of flapping design parameters. (A) model of the flapping wing showing the design parameter definition. (B) Multi-objective optimization procedure based on NSGA-II method. (C) Optimization results.

local attack angle α_{local} is composed of the installation angle α_0 and reverse angle α_s (as shown in Fig3(A)):

$$\alpha_{local} = \begin{cases} \alpha_0 - 0.5\alpha_s, & downward - flapping \\ \alpha_0 - 0.5\alpha_s, & upward - flapping \end{cases} \tag{5}$$

Besides, to estimate the force on each strip, quasi-steady aerodynamic model is used in our work [6], [31], [32] owing to the time and computational resource requirements of the optimization work. In the quasi-steady aerodynamic model, the total aerodynamic force can be divided into lift force L and drag force D, and the function of dimensionless coefficients C_L and C_D can be obtained by fitting the experimental results [31]:

$$\begin{aligned} C_L(\alpha_{local}) &= C_{L_{\max}} \sin(2\alpha_{local}) \\ C_D(\alpha_{local}) &= \left(\frac{C_{D_{\max}} + C_{D_0}}{2}\right) - \left(\frac{C_{D_{\max}} - C_{D_0}}{2}\right)\cos(2\alpha_{local}) \end{aligned} \tag{6}$$

in which, $C_{L_{\max}} = 1.8$, $C_{D_0} = 0.4$, $C_{D_{\max}} = 3.4$.

Based on the aerodynamic model of the dragonfly-inspired flapping wing. The objective function of lift force and energy consumption can be stated as follows:

Objective functions:

$$\begin{cases} \max L = \int_0^R \frac{1}{2}\rho v_{local}^2 C_L(\alpha_{local}) C(r) \mathrm{d}r \\ \min E = \int_0^R \frac{1}{2}\rho v_{local}^3 C_D(\alpha_{local}) C(r) r \mathrm{d}r \end{cases} \tag{7}$$

C. Multiobjective Optimization based on NSGA Method

NSGA-II [33] (Fig. 3(B)) method is selected to solve the multi objective optimization problem aiming at the biggest lift force and lowest energy consumption of the dragonfly-inspired flapping motion under 20Hz flapping frequency, and the results are plotted in Fig. 3(C). The optimization results show that in hovering situation, the desired installation angle $\alpha_0 = 0°$, and the desired wing reverse angle $\alpha_s = 90°$. Such an optimization algorithm framework could be further implemented to find other desired design parameters of the DFWR, such as in forward flight under different velocities.

IV. Inclined-Stroke-Plane Control Approach

In this section, in order to further validate the feasibility of the tiltable flapping mechanism in practical applications, force and torque experiments of an integrated module are conducted. In addition, a quasi-steady aerodynamic model is also established to estimate the control moment produced by the tiltable flapping mechanism.

A. Theoretical Model

As shown in Fig. 4, the attitude of DFWR could be fully controlled by tilting the stroke plane with four independent servo motors.

When the robot needs to produce a pitching moment for flying forward or backward, the stroke planes of two wings in the same module are rotated to the same direction as shown in Fig. 4A. The yaw control is produced through asymmetric tilting angle between wings on the left and right side as shown in Fig. 4B. Similarly, the asymmetric rotation of the right and left wings will also results in a difference in upward forces. Hence, the roll control could be realized by tilting one side

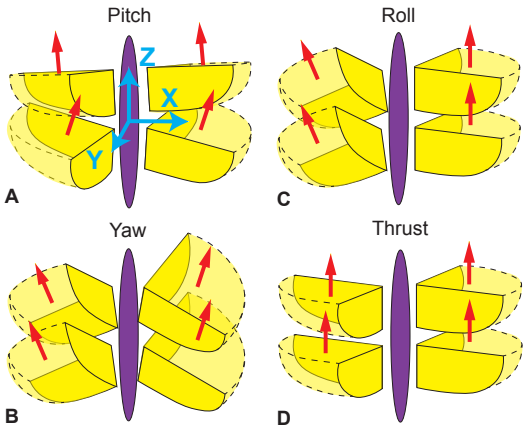

Fig. 4. Concept of the tiltable stroke plane modulation of the proposed DFWR for pitch, roll, yaw, and thrust control.

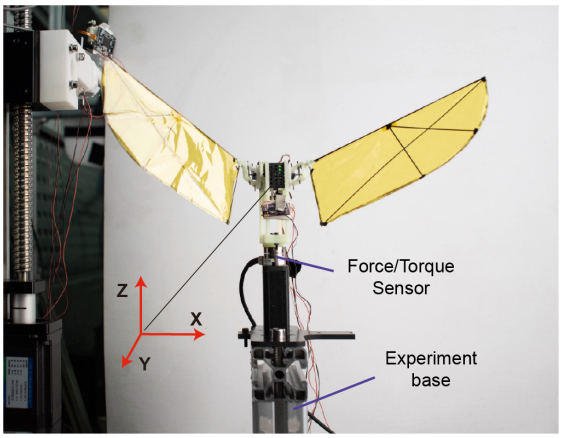

Fig. 5. Experimental setup and coordinate of the "force vector" flapping mechanism. The forces and torques are measured by a 6-axis load sensor.

stroke plane of the wings. Figure 4C shows that for a left-side turn, the left forewing and hindwing rotate a positive tilting angle $+\delta_{fl}, +\delta_{hl}$, which will produce a positive rolling moment.

Based on the above control strategy, the 3-axis control moment around the body frame can be written as the function of tilting angle $\delta_{fl}, \delta_{fr}, \delta_{hl}, \delta_{hr}$

$$\tau_x = \bar{F}_L D(\sin\delta_{fl} + \sin\delta_{fr} - \sin\delta_{hl} - \sin\delta_{hr}) \quad (8)$$

$$\tau_y = \bar{F}_L L(\cos\delta_{fl} - \cos\delta_{fr} + \cos\delta_{hl} - \cos\delta_{hr}) \quad (9)$$

$$\tau_z = \bar{F}_L L(\sin\delta_{fl} - \sin\delta_{fr} + \sin\delta_{hl} - \sin\delta_{hr}) \quad (10)$$

where $\bar{F}_L$ is the average lift force of the flapping wing. D is the distance between the wing root and the center of gravity in the side view, which is half of the distance between the wing root of forewings and hindwings. L is the equivalent moment arm of the distributed lift force acting on the wing. According to the quasi-steady aerodynamic model, this value can be estimated by dividing aerodynamic moment M_y with lift force F_L, as the following

$$L = \frac{M_y}{F_L} = \frac{0.5\rho\dot{\phi}^2 C_L \int_0^R r^3 c(r) r dr}{0.5\rho\dot{\phi}^2 C_L \int_0^R r^2 c(r) dr} \quad (11)$$

where ρ is the air density, $\dot{\phi}$ is flapping angular velocity, C_L is lift coefficient as given in equation (6), r is the span-wise location of a strip used for integration, $c(r)$ is the chord length at location r. According to [34], the kth power of non-dimensional radius of the kth moment of wing area is given by

$$\hat{r}_k^k = \frac{\int_0^R c(r) r^k \mathrm{d}r}{SR^k}, k = 1, 2, 3 \quad (12)$$

where $S = \int_0^R c(r)\mathrm{d}r$ is the wing area. Hence, the equivalent moment arm of the aerodynamic moment M_x can be written into

$$L = R\hat{r}_3^3/\hat{r}_2^2 \quad (13)$$

Based on the given chord distribution in equation (3), the non-dimensional radius of the first and second moment of wing area are calculated respectively. These values are listed in table II.

B. Experimental Setup

To quantify the control torque of the proposed tiltable flapping wing mechanism, the force/torque experiment was conducted by using a single module (half of the whole robot). The geometry parameters of the flapping wing are the same as given in table II.

As shown in Fig. 5, the integrated flapping wing mechanism was fixed on the sensor through a 3D-printed connector, and enough space was reserved to avoid the ground effects. The upward forces and torque are measured by a 6-axis force/torque sensor (Nano 17, ATI Industrial Automation), which has a force resolution of 3 mN and torque resolution of 0.016 mNm. Signals from the transducer were transmitted to the computer via a data acquisition board (NI-USB6280) with a sampling frequency of 2 KHz. The periodical force and torque data are averaged over 4 seconds to estimate the mean value in one flapping cycle.

During the experiments, the tilting angle of the left and right wings' stroke plane was tuned by two servo motors respectively, which were controlled by receiving the PWM signals from an Arduino UNO board. The speed of the BLDC motor was adjusted by an electrical speed controller(ESC, max current 6A), which was powered by a constant voltage of 8V.

C. Experimental Results

The validation experiments are divided into a pitching moment experiment and a yaw moment experiment. In the test, the throttle of the BLDC motor is fixed at 40%, which resulting a flapping frequency of 8Hz and an average lift about 0.11N.

In the pitch torque experiment, the two servo motors have a synchronized tilting angle from 0 degree to 30 degree. As shown in Fig. 6A and B, a maximum pitching moment of -3.8Nmm could be generated at 30-degree tilting angle. And the upward lift force in Z direction slightly decreased from 0.11N to 0.095N. In addition, the experimentally measured results are consistent with the trends predicted based on equations (8) to (13).

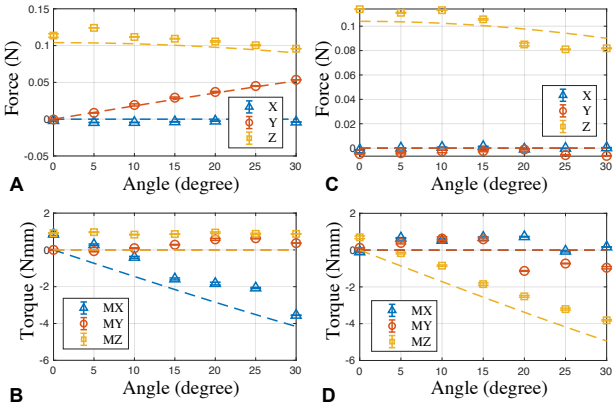

Fig. 6. Average force and torque measurement results with predicted values at different tilting angles. (A)(B) Forces and moments when the two wings tilting to the same direction to generate a pitch control moment. (C)(D) Forces and moments when the two wings tilting to the opposite direction to generate a yaw control moment.

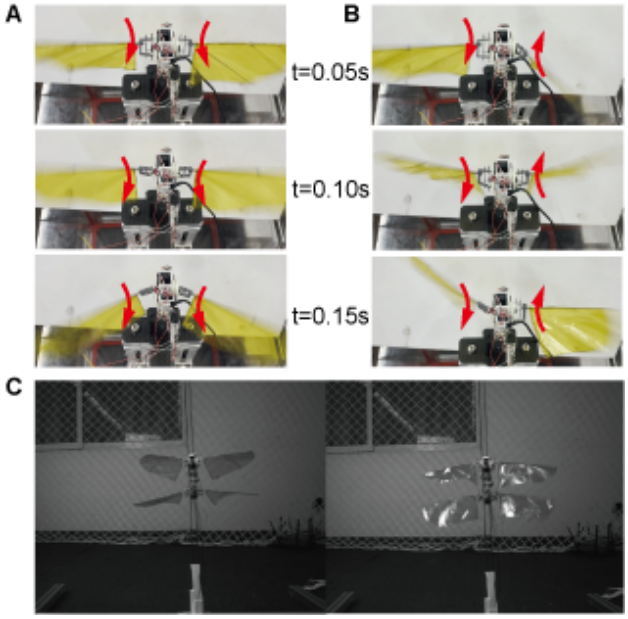

Fig. 7. Operation performance demonstration of DFWR. The operation of the "force vectoring" mechanism in synchronous rotation (A) and asynchronous rotation (B) under high-speed flapping motion. (C) Guided flight test of the DFWR prototype.

In the yaw torque experiment, the tilting angles produced by the left and right servos are equal in magnitude, but in opposite directions. As shown in Fig. 6D, the yaw torque (MZ) corresponds well with the predicted value calculated in Section IV A. When tilting at 30 degrees oppositely, the two wings could achieve an average yaw control moment of -3.9 Nmm. As shown in Fig. 6C, the upward force (Z) could also slightly decrease due to the rotation of the force vector. As for the roll torque, it is coupled with yaw by deploying the control strategy as shown in Fig. 4, and can be estimated through equation (8).

V. Operation Validation

A. Validation of "force vectoring" mechanism

In our proposed DFWR platform, the "force vectoring" control approach is mainly achieved by four servos. Previous experiments in Section. IV have demonstrated that the servos can hold a fixed inclined angle during flapping motion. Here, added operation tests (Fig. 7A and B) including a synchronous rotation test and an asynchronous rotation test are conducted to verify the dynamic response of the servos under high-speed flapping motion (10Hz).

B. Guided flight test

The objective of the guided takeoff test is to assess the feasibility of integrating the tiltable flapping wing mechanism onto the robotic platform. Specifically, it aims to verify the mechanism's capability to generate an adequate amount of lift and ensure seamless interfacing between the forewing and hindwing components.

A high-speed camera (500fps) was used to record its trajectory and flapping frequency, and a DC current clamp (CC65, Hantek, resolution 10 mA) was used to measure the net current during the experiments. During the experiment, the 140mm wingspan prototype was powered by a voltage of 8.4V and an 80% throttle. The total weight of the prototype is 36.6 grams (without accounting for the wires). As shown in Fig. 7C, when the DFWR flies at a flapping frequency of 13Hz, the average current of the two motors is about 0.40A, resulting in a power consumption of 3.36W. The lift-to-power ratio of the robot could reach up to 10.89 gf/W.

VI. Conclusion and Future Work

To mimic the great maneuverability of dragonflies shown in their backward flight, we have designed and fabricated a dragonfly-inspired tandem flapping wing robotic platform, DFWR. Taking inspiration from dragonflies' "force vectoring" control mechanism reported in the literature, the implementation of the DFWR platform includes (i) design of the DFWR platform in tandem flapping wing configuration, giving it four stroke-plane inclination control degrees; (ii) multi-objective optimization of the flapping wing based on NSGA-II method, considering both the power consumption and total lift during flapping motion; (iii) theoretical deviation and experimental test on the control torque of the proposed platform, verifying the control logic and sufficient control torque; (iv) operation verification including a "force vectoring" mechanism test and guided flight test, to ensure the design feasibility under high-speed flapping motion.

Considering that one target application of our proposed DFWR is to further help comprehension of the flight and maneuver of Odonata, some essential aspects should be further enhanced before translating the DFWR into field operations. On the one hand, the current prototype needs further structural weight reduction optimization, aiming for a thrust-to-weight ratio of 1.5 or more. On the other hand, the fore-hind wing needs a flapping phase coupling to avoid the forewing-hindwing flapping interference, which could be achieved by using the same actuating motor.

References

[1] D. Floreano and R. J. Wood, "Science, technology and the future of small autonomous drones," *nature*, vol. 521, no. 7553, pp. 460–466, 2015.

[2] Y. Chen, H. Wang, E. F. Helbling, N. T. Jafferis, R. Zufferey, A. Ong, K. Ma, N. Gravish, P. Chirarattananon, M. Kovac *et al.*, "A biologically inspired, flapping-wing, hybrid aerial-aquatic microrobot," *Science robotics*, vol. 2, no. 11, p. eaao5619, 2017.

[3] R. Wood, R. Nagpal, and G.-Y. Wei, "Flight of the robobees," *Scientific American*, vol. 308, no. 3, pp. 60–65, 2013.

[4] G. C. De Croon, M. Groen, C. De Wagter, B. Remes, R. Ruijsink, and B. W. van Oudheusden, "Design, aerodynamics and autonomy of the delfly," *Bioinspiration & biomimetics*, vol. 7, no. 2, p. 025003, 2012.

[5] M. Keennon, K. Klingebiel, and H. Won, "Development of the nano hummingbird: A tailless flapping wing micro air vehicle," in *50th AIAA aerospace sciences meeting including the new horizons forum and aerospace exposition*, 2012, p. 588.

[6] M. H. Dickinson, F.-O. Lehmann, and S. P. Sane, "Wing rotation and the aerodynamic basis of insect flight," *Science*, vol. 284, no. 5422, pp. 1954–1960, 1999.

[7] M. Sun, "High-lift generation and power requirements of insect flight," *Fluid Dynamics Research*, vol. 37, no. 1-2, p. 21, 2005.

[8] Z. Tu, F. Fei, J. Zhang, and X. Deng, "An at-scale tailless flapping-wing hummingbird robot. I. Design, optimization, and experimental validation," *IEEE Transactions on Robotics*, vol. 36, no. 5, pp. 1511–1525, 2020.

[9] F. Fei, Z. Tu, and X. Deng, "An at-scale tailless flapping wing hummingbird robot. II. Flight control in hovering and trajectory tracking," *Bioinspiration & Biomimetics*, vol. 18, no. 2, p. 026003, 2023.

[10] H. V. Phan, T. Kang, and H. C. Park, "Design and stable flight of a 21 g insect-like tailless flapping wing micro air vehicle with angular rates feedback control," *Bioinspiration & biomimetics*, vol. 12, no. 3, p. 036006, 2017.

[11] M. Karásek, F. T. Muijres, C. De Wagter, B. D. Remes, and G. C. De Croon, "A tailless aerial robotic flapper reveals that flies use torque coupling in rapid banked turns," *Science*, vol. 361, no. 6407, pp. 1089–1094, 2018.

[12] A. Chen, B. Song, Z. Wang, D. Xue, and K. Liu, "A novel actuation strategy for an agile bioinspired FWAV performing a morphing-coupled wingbeat pattern," *IEEE Transactions on Robotics*, vol. 39, no. 1, pp. 452–469, 2022.

[13] R. J. Bomphrey, T. Nakata, P. Henningsson, and H.-T. Lin, "Flight of the dragonflies and damselflies," *Philosophical Transactions of the Royal Society B: Biological Sciences*, vol. 371, no. 1704, p. 20150389, 2016.

[14] N. Gaissert, R. Mugrauer, G. Mugrauer, A. Jebens, K. Jebens, and E. M. Knubben, "Inventing a micro aerial vehicle inspired by the mechanics of dragonfly flight," in *Towards Autonomous Robotic Systems: 14th Annual Conference, TAROS 2013, Oxford, UK, August 28–30, 2013, Revised Selected Papers 14*. Springer, 2014, pp. 90–100.

[15] J. Ratti and G. Vachtsevanos, "Inventing a biologically inspired, energy efficient micro aerial vehicle," *Journal of Intelligent & Robotic Systems*, vol. 65, pp. 437–455, 2012.

[16] Y. Chen, C. Arase, Z. Ren, and P. Chirarattananon, "Design, characterization, and liftoff of an insect-scale soft robotic dragonfly powered by dielectric elastomer actuators," *Micromachines*, vol. 13, no. 7, p. 1136, 2022.

[17] G. Rüppell and D. Hilfert-Rüppell, "Rapid acceleration in odonata flight: highly inclined and in-phase wing beating," *International Journal of Odonatology*, vol. 23, no. 1, pp. 63–78, 2020.

[18] Z. J. Wang, J. Melfi Jr, and A. Leonardo, "Recovery mechanisms in the dragonfly righting reflex," *Science*, vol. 376, no. 6594, pp. 754–758, 2022.

[19] N. Sapir and R. Dudley, "Backward flight in hummingbirds employs unique kinematic adjustments and entails low metabolic cost," *Journal of Experimental Biology*, vol. 215, no. 20, pp. 3603–3611, 2012.

[20] A. T. Bode-Oke, S. Zeyghami, and H. Dong, "Strategies for achieving backward flight by a dragonfly," in *30th Congress of the International Council of the Aeronautical Sciences*, 2016.

[21] S. Bode-Oke.Ayodeji T, Zeyghami and H. Dong, "Flying in reverse: kinematics and aerodynamics of a dragonfly in backward free flight," *Journal of The Royal Society Interface*, vol. 15, no. 143, p. 20180102, 2018.

[22] S. Singh, M. Zuber, M. N. Hamidon, N. Mazlan, A. A. Basri, and K. A. Ahmad, "Classification of actuation mechanism designs with structural block diagrams for flapping-wing drones: A comprehensive review," *Progress in Aerospace Sciences*, vol. 132, p. 100833, 2022.

[23] H. V. Phan and H. C. Park, "Insect-inspired, tailless, hover-capable flapping-wing robots: Recent progress, challenges, and future directions," *Progress in Aerospace Sciences*, vol. 111, p. 100573, 2019.

[24] Z. Tu, F. Fei, and X. Deng, "Bio-inspired rapid escape and tight body flip on an at-scale flapping wing hummingbird robot via reinforcement learning," *IEEE Transactions on Robotics*, vol. 37, no. 5, pp. 1742–1751, 2021.

[25] F. Liu, S. Li, Z. Wang, X. Dong, D. Li, and Z. Tu, "Liftoff of a motor-driven flapping wing rotorcraft with mechanically decoupled wings," in *2022 International Conference on Robotics and Automation (ICRA)*. IEEE, 2022, pp. 2092–2098.

[26] R. McGill, N.-s. P. Hyun, and R. J. Wood, "Frequency-modulated control for insect-scale flapping-wing vehicles," *IEEE Robotics and Automation Letters*, vol. 7, no. 4, pp. 12 515–12 522, 2022.

[27] R. M. Bena, X. Yang, A. A. Calderón, and N. O. Pérez-Arancibia, "High-performance six-dof flight control of the bee: An inclined-stroke-plane approach," *IEEE Transactions on Robotics*, vol. 39, no. 2, pp. 1668–1684, 2023.

[28] X. Liu, C. Hefler, W. Shyy, and H. Qiu, "The importance of flapping kinematic parameters in the facilitation of the different flight modes of dragonflies," *Journal of Bionic Engineering*, vol. 18, no. 2, pp. 419–427, 2021.

[29] X. Liu, C. Hefler, J. Fu, W. Shyy, and H. Qiu, "Implications of wing pitching and wing shape on the aerodynamics of a dragonfly," *Journal of Fluids and Structures*, vol. 101, p. 103208, 2021.

[30] C. Li and H. Dong, "Wing kinematics measurement and aerodynamics of a dragonfly in turning flight," *Bioinspiration & biomimetics*, vol. 12, no. 2, p. 026001, 2017.

[31] J. P. Whitney and R. J. Wood, "Aeromechanics of passive rotation in flapping flight," *Journal of fluid mechanics*, vol. 660, pp. 197–220, 2010.

[32] X. Ke, W. Zhang, X. Cai, and W. Chen, "Wing geometry and kinematic parameters optimization of flapping wing hovering flight for minimum energy," *Aerospace science and Technology*, vol. 64, pp. 192–203, 2017.

[33] K. Deb, A. Pratap, S. Agarwal, and T. Meyarivan, "A fast and elitist multiobjective genetic algorithm: NSGA-II," *IEEE transactions on evolutionary computation*, vol. 6, no. 2, pp. 182–197, 2002.

[34] C. Ellington, "The aerodynamics of insect flight. II. morphological parameters," *Phil. Trans. R. Soc. Lond. B*, vol. 305, pp. 17–40, 1984.